

# Two-loop QED/QCD corrections for polarized $\gamma\gamma \rightarrow \gamma\gamma$ process in SANCPHOT

S.G. Bondarenko<sup>1</sup>\*, A. Issadykov<sup>1,3</sup>, L.V. Kalinovskaya<sup>2</sup>, A.A. Sapronov<sup>2</sup>, D. Seitova<sup>3</sup>

<sup>1</sup> *Bogoliubov Laboratory of Theoretical Physics, JINR, Dubna, 141980 Russia*

<sup>2</sup> *Dzhelepow Laboratory of Nuclear Problems, JINR, Dubna, 141980 Russia*

<sup>3</sup> *Institute for Nuclear Physics, Ministry of Energy of the Republic of Kazakhstan, Almaty, 050032, Kazakhstan*

## Abstract

The new version of the SANCPHOT integrator has been prepared for fast and stable numerical calculations up to two loops for polarized light-by-light scattering. One-loop modules based on the helicity formalism with massive particles and two-loop modules with massless particles inside the loops are used. The presented study is driven by the potential of polarized photon beams to probe the high energy region. This study is a contribution to the research program of the CEPC project being under development in China.

**Keywords:** light-by-light, polarization, QED, QCD, radiative corrections

## 1 Introduction

Further studies of light-by-light (LbL) scattering

$$\gamma(p_1) + \gamma(p_2) \rightarrow \gamma(p_3) + \gamma(p_4),$$

are mainly related to the high-luminosity  $e^+e^-$  colliders (FCC<sub>ee</sub> [1, 2], CEPC [3, 4, 5], ILC [6, 7], CLIC [8, 9, 10, 11]) and optionally to the collider at low energies (Genie in China [12]). In both cases, the highly polarized initial state photons are created through the photon production during the laser Compton backscattering process off the high energy electron beam. The idea of observation of polarized  $\gamma\gamma$  collisions at linear colliders via Compton backscattering was proposed by the Novosibirsk group [13, 14, 15]. Polarized photon beams, large cross sections and high luminosity allow one to significantly improve the accuracy of measurements at photon colliders and thus should naturally be included into theoretical calculations and corresponding codes.

In 2017, the ATLAS and CMS Collaborations at the LHC performed the first measurement of LbL scattering in heavy-ion collisions [16, 17, 18]. From the theoretical side, this experiment was supported by the codes SuperChic 4 [19] and GAMMA-UPC+MadGraph5\_aMC@NLO [20, 21] at the one-loop level. The theoretical estimation of the cross sections comprised about two standard deviations below the ATLAS measured value. Consequently, for the modern highest experimental accuracy of a similar experiment, corrections with a higher than one-loop level of perturbative approximation are vitally needed.

For low-energy applications, the world's first gamma-photon collider, Genie (Qini), is set to be developed. This collider aims to conduct direct experimental tests on light-by-light scattering, focusing on

---

\*E-mail: bondarenko@jinr.ru

achieving the maximum cross section at a center-of-mass energy of 1-2 MeV [12]. The theoretical framework will be supported by the CAIN 2.42 code [22, 23]. In the MeV energy range, it is crucial to apply a specific limit for helicity, as all amplitudes with an odd number of positive helicities vanish in the low-energy limit. This vanishing occurs at all-loop orders. However, for experiments like Genie, it is essential to consider the massive case. In the near future, we are planning to calculate the low-energy limit for the massive case of two-loop helicity.

The previous version of SANCphot integrator [24] was intended for calculations of the processes  $\gamma\gamma \rightarrow \gamma\gamma(\gamma Z, ZZ)$  at the one-loop precision level. In the SANC project [25], helicity formalism was always used. In this approach it is easy to add higher-order corrections and it is extremely convenient to estimate polarization [26, 27]. This paper provides a description of the new version of the SANCphot integrator for fast and stable numerical calculations up to two QED/QCD loops for LbL scattering. The current version is adjusted to study the two-loop results in the ultra-relativistic limit (kinematic invariants  $s, t, u$  are much greater than the squared masses of charged fermions) in addition to SANC one-loop level calculations with massive particles [28, 29] inside the loops. The expressions for two-loop amplitudes in terms of fermion loops correspond to the massless QCD- and QED-case [30].

The two-loop corrections to LbL scattering were computed two decades ago [30, 31]. In these works, the massless amplitudes were considered, as they are deemed to be most computationally accessible. Recently, the two-loop massive QCD and QED helicity amplitudes for light-by-light scattering were presented in [32, 33].

This article consists of four Sections. The implementation of the two-loop QED/QCD corrections for polarized LbL cross sections within the helicity approach is described in Section 2. In Section 3 we present a comparison and numerical results. Finally, the summary is given in Section 4.

## 2 Contribution of the two-loop QED/QCD corrections

In this section, a short explanation of the implementation of two-loop QED/QCD corrections by using the helicity amplitudes is presented.

The basic set of two-loop diagrams consists of three types of nonvanishing Feynman diagrams corresponding to the connection of any two sides of the box with the photon QED or gluon QCD propagator; see Fig. (1). The complete numbers of sixty nonvanishing Feynman diagrams are obtained by all possible permutations. All other types of QCD diagrams vanish by Furry's theorem or simple group theory.

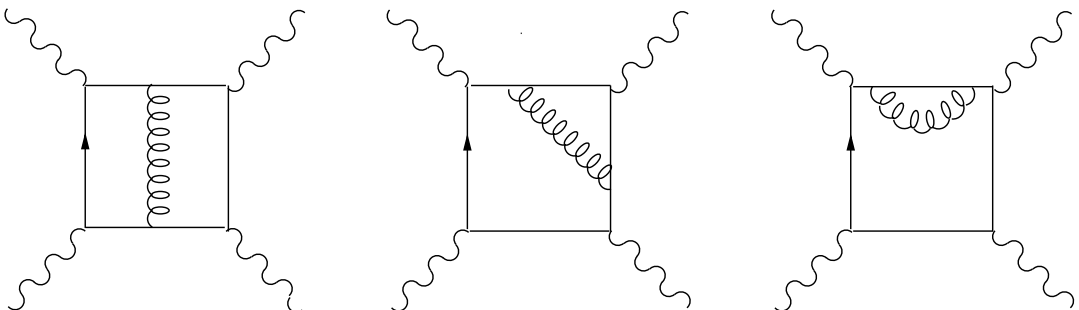


**Fig. 1.** Two-loop diagrams corresponding to internal photon/gluon exchange

The QCD- and QED-corrected two-loop amplitudes are given by the following expressions [30]:

$$\mathcal{H}_{\lambda_1\lambda_2\lambda_3\lambda_4}^{\text{2-loop, QCD(QED)}} = N^{\text{QCD(QED)}} \mathcal{H}_{\lambda_1\lambda_2\lambda_3\lambda_4}^{(2)} \quad (1)$$

with the coefficients  $N^{\text{QCD}} = 4(N^2 - 1)Q^4\alpha^2 \frac{\alpha_s(\mu)}{\pi}$ , and  $N^{\text{QED}} = 8NQ^6\alpha^2 \frac{\alpha(\mu)}{\pi}$ , where  $N$  is the fermion color factor (3 for quarks, 1 for leptons), and  $Q$  is the fermion charge in units of  $e$ .

### 3 Polarized photon beams

Taking into account parity invariance and Bose statistics, the cross section of polarized LbL scattering in a simplified form was derived in [26, 27], and we use it in our calculations [24].

The expressions for the helicity amplitudes  $\mathcal{H}^{(2)}$  in the  $m_f = 0$  limit (where  $m_f$  is the fermion mass in a loop) are given in [30]. Equation (1) from [24] is used to calculate the contributions of one and two loops to the polarized cross section. The helicity amplitudes in the equation are:

$$\mathcal{H} = \mathcal{H}^{\text{1-loop}} + \mathcal{H}^{\text{2-loop, QCD(QED)}}.$$

In the calculations, the square of the  $\mathcal{H}^{\text{2-loop}}$  amplitude was omitted as part of the higher-order corrections.

### 4 SANCPHOT numerical results

The numerical results for LbL scattering contain estimates of the total cross sections and different final state kinematic distributions at fixed incoming electron beam energies

$$\sqrt{s} = 250, 500, 1000 \text{ GeV} \quad (2)$$

and various polarization setups.

The numerical validation was performed in the  $\alpha(0)$  EW scheme using the setup given below:

$$\begin{aligned} \alpha &= 1/137.035990996, & \alpha_s &= 0.176, \\ M_W &= 80.45149 \text{ GeV}, & M_Z &= 91.18670 \text{ GeV}, \\ M_H &= 125 \text{ GeV}, \\ m_e &= 0.51099907 \text{ MeV}, & m_\mu &= 0.105658389 \text{ GeV}, \\ m_\tau &= 1.77705 \text{ GeV}, \\ m_u &= 0.062 \text{ GeV}, & m_d &= 0.083 \text{ GeV}, \\ m_c &= 1.5 \text{ GeV}, & m_s &= 0.215 \text{ GeV}, \\ m_t &= 173.8 \text{ GeV}, & m_b &= 4.7 \text{ GeV}. \end{aligned}$$

The cross section has been integrated over a range of center-of-mass scattering angles  $|\theta| > 30^\circ$ .

To verify the technical precision of our codes, the results shown in Fig. 3 of [30] for various quantities  $k$  (see the definition (3.4)) were repeated. For unpolarized initial and final photons and fully polarized (++) and (++) initial photons, a good agreement was observed. Qualitative agreement with the results in Fig. 4 for the QCD correction was also obtained.

In order to probe the dependence of the total cross section on the initial polarizations, the numerical tests were conducted using the same three polarization combinations as in [24]:

$$\begin{aligned} \text{set 1 : } & P_e = P'_e = 0.8, \\ & P_\gamma = P'_\gamma = -1, P_t = P'_t = 0, \\ \text{set 2 : } & P_e = P'_e = 0, P_\gamma = P'_\gamma = 0, \\ & P_t = P'_t = 1, \phi = \pi/2, \\ \text{set 3 : } & P_e = 0.8, P'_e = 0, P_\gamma = -1, P'_\gamma = 0, \\ & P_t = 0, P'_t = 1, \phi = \pi/2, \end{aligned} \quad (3)$$

where  $P_e$ ,  $P_\gamma$  and  $P'_\gamma$  denote the helicities of the initial electron, laser and scattered photon [34]. We consider three cases for laser photons when either both laser photons are purely transversely polarized, i.e.  $P_t = P'_t = 1$  or only one of them is polarized, forward or backward.

## 4.1 Cross section

The corresponding results for the total cross section for polarized LbL are presented in Table 1 where the relative corrections  $\delta$  are computed as the ratios (in percent) of the corresponding radiative corrections (QED/QCD) to the LO level cross section, i.e.  $\delta = \sigma^{\text{NLO}}/\sigma^{\text{LO}} - 1$  where LO stands for 1-loop, and NLO – for 2-loop contributions.

The sign and magnitude of the integrated relative corrections corresponding to the QED and QCD two-loop effects strongly depend on the energy and polarization combination. The QED contributions are usually only 10% of the QCD ones, which can easily be obtained from the ratio  $N^{\text{QED}}/N^{\text{QCD}}$ . The magnitude of the relative corrections for set 1 is smaller than for sets 2 and 3. For center-of-mass energy  $\sqrt{s_{ee}} = 250$  GeV the magnitude of the relative QCD corrections is approximately 0.2 % for set 1 and approximately  $(-0.4)$ – $(-0.5)$  % for sets 2, 3. For  $\sqrt{s_{ee}} = 500$  GeV the magnitude of the relative QCD corrections is  $(-0.4)$  % for set 1 and  $(-1)$  % for sets 2, 3. For  $\sqrt{s_{ee}} = 1000$  GeV the magnitude of the relative QCD corrections is approximately  $(-0.7)$  % for set 1 and  $(-0.9)$  % for sets 2, 3. Thus, these contributions are rather large under the requirements for modern experimental precision.

**Table 1.** Integrated one-loop cross sections  $\sigma(\gamma\gamma)$  [fb] and the corresponding relative corrections  $\delta$  [%] for the process  $\gamma\gamma \rightarrow \gamma\gamma$  in different polarization setups

| $\sqrt{s_{ee}}$ |                           | 250 GeV   | 500 GeV   | 1 TeV     |
|-----------------|---------------------------|-----------|-----------|-----------|
| set 1           | $\sigma$ , fb             | 22.524(1) | 9.445(1)  | 6.940(1)  |
|                 | $\delta^{\text{QED}}, \%$ | 0.017(6)  | -0.039(3) | -0.062(3) |
|                 | $\delta^{\text{QCD}}, \%$ | 0.184(6)  | -0.415(3) | -0.662(3) |
| set 2           | $\sigma$ , fb             | 24.426(1) | 8.045(1)  | 6.861(1)  |
|                 | $\delta^{\text{QED}}, \%$ | -0.038(6) | -0.099(2) | -0.087(3) |
|                 | $\delta^{\text{QCD}}, \%$ | -0.406(6) | -1.052(2) | -0.927(2) |
| set 3           | $\sigma$ , fb             | 22.320(1) | 8.014(1)  | 6.7967(1) |
|                 | $\delta^{\text{QED}}, \%$ | -0.042(6) | -0.103(2) | -0.084(2) |
|                 | $\delta^{\text{QCD}}, \%$ | -0.444(6) | -1.101(2) | -0.900(2) |

## 4.2 Differential distributions

Figure 2 shows the main final-state kinematic distributions  $\cos \vartheta$ ,  $M_{\text{inv}}$  and  $p_T$  for polarized LbL scattering for three different initial electron energies (2) and three combinations of the initial beams polarization (3).

The upper panels show the two-loop contributions of QED and QCD to the polarized cross sections with sets (3). The lower panels show the relative corrections of the QED/QCD two-loop contributions in parts.

The behavior of the relative correction distributions strongly depends on the energy and polarization combinations.

The results for the relative correction distributions on  $\cos \theta$  for set 1 at  $\sqrt{s_{ee}} = 250$  GeV are mainly positive, while the corrections for all other energies and sets are negative.

The relative corrections for the invariant mass  $M_{\text{inv}}$  distributions range from  $-2.5\%$  to  $1\%$  for center-of-mass energies  $\sqrt{s_{ee}} = 250, 500$  GeV. For  $\sqrt{s_{ee}} = 1000$  GeV, the range widens from  $-4\%$  to  $1.5\%$ . The relative corrections for the transverse momentum  $p_t$  distributions exhibit similar behavior and magnitude as those observed for the invariant mass  $M_{\text{inv}}$  distributions. In summary, the corrections for  $p_t$  follow a pattern comparable to that for  $M_{\text{inv}}$ .

## 5 Summary

The latest version of `SANCphot` has been adapted to study polarized LbL scattering. It incorporates electroweak one-loop radiative corrections to realistic observables, as well as QCD/QED two-loop corrections that are relevant for the LbL process.

The two-loop QED/QCD corrections make a substantial contribution.

Including contributions up to the two-loop level, along with mass effects, allows a high degree of precision in the theoretical predictions for LbL scattering. Achieving this level of precision is essential to align with the anticipated experimental accuracy in future measurements.

## 6 Funding

This research has been funded by the Committee of Science of the Ministry of Science and Higher Education of the Republic of Kazakhstan (Grant No. AP19680084).

## References

- [1] FCC-ee homepages — <http://tlep.web.cern.ch>.
- [2] FCC Collaboration, A. Abada *et al.*, *Eur. Phys. J. ST* **228** (2019), no. 2 261–623.
- [3] CEPC homepages — <http://cepc.ihep.ac.cn/intro.html>.
- [4] CEPC Study Group Collaboration, M. Dong *et al.*, [1811.10545](https://arxiv.org/abs/1811.10545).
- [5] CEPC Study Group Collaboration, W. Abdallah *et al.*, *Radiat. Detect. Technol. Methods* **8** (2024), no. 1 1–1105, [2312.14363](https://arxiv.org/abs/2312.14363).
- [6] ILC homepages — <https://www.linearcollider.org/ILC>.
- [7] ILC Collaboration, [1306.6352](https://arxiv.org/abs/1306.6352).
- [8] CLIC homepages — <http://clic-study.web.cern.ch>.
- [9] CLICdp, CLIC Collaboration, T. K. Charles *et al.*, [1812.06018](https://arxiv.org/abs/1812.06018).
- [10] CLICdp, ILD concept group Collaboration, A. F. Zarnecki, *PoS CORFU2019* (2020) 037, [2004.14628](https://arxiv.org/abs/2004.14628).
- [11] O. Brunner *et al.*, [2203.09186](https://arxiv.org/abs/2203.09186).
- [12] T. Takahashi *et al.*, *Eur. Phys. J. C* **78** (2018), no. 11 893, [Erratum: *Eur.Phys.J.C* 82, 404 (2022)], [1807.00101](https://arxiv.org/abs/1807.00101).
- [13] I. F. Ginzburg, G. L. Kotkin, V. G. Serbo, and V. I. Telnov, *JETP Lett.* **34** (1981) 491–495.
- [14] I. F. Ginzburg, G. L. Kotkin, V. G. Serbo, and V. I. Telnov, *Nucl. Instrum. Meth.* **205** (1983) 47–68.
- [15] I. F. Ginzburg, G. L. Kotkin, S. L. Panfil, V. G. Serbo, and V. I. Telnov, *Nucl. Instrum. Meth. A* **219** (1984) 5–24.
- [16] ATLAS Collaboration, M. Aaboud *et al.*, *Nature Phys.* **13** (2017), no. 9 852–858, [1702.01625](https://arxiv.org/abs/1702.01625).
- [17] CMS Collaboration, A. M. Sirunyan *et al.*, *Phys. Lett. B* **797** (2019) 134826, [1810.04602](https://arxiv.org/abs/1810.04602).

[18] ATLAS Collaboration, G. Aad *et al.*, *JHEP* **03** (2021) 243, [Erratum: *JHEP* 11, 050 (2021)], [2008.05355](#).

[19] L. A. Harland-Lang, M. Tasevsky, V. A. Khoze, and M. G. Ryskin, *Eur. Phys. J. C* **80** (2020), no. 10 925, [2007.12704](#).

[20] H.-S. Shao and D. d'Enterria, *JHEP* **09** (2022) 248, [2207.03012](#).

[21] J. Alwall, R. Frederix, S. Frixione, V. Hirschi, F. Maltoni, O. Mattelaer, H. S. Shao, T. Stelzer, P. Torrielli, and M. Zaro, *JHEP* **07** (2014) 079, [1405.0301](#).

[22] P. Chen, T. Ohgaki, A. Spitkovsky, T. Takahashi, and K. Yokoya, *Nucl. Instrum. Meth. A* **397** (1997) 458–464, [physics/9704012](#).

[23] K. Yokoya, *User manual of CAIN, version 2.40* (2018).

[24] S. G. Bondarenko, L. V. Kalinovskaya, and A. A. Sapronov, *Comput. Phys. Commun.* **294** (2024) 108929, [2201.04350](#).

[25] A. Andonov, A. Arbuzov, D. Bardin, S. Bondarenko, P. Christova, L. Kalinovskaya, G. Nanava, and W. von Schlippe, *Comput. Phys. Commun.* **174** (2006) 481–517, [Erratum: *Comput.Phys.Commun.* 177, 623–624 (2007)], [hep-ph/0411186](#).

[26] G. J. Gounaris, P. I. Porfyriadis, and F. M. Renard, *Phys. Lett. B* **452** (1999) 76–82, [Erratum: *Phys.Lett.B* 513, 431–431 (2001), Erratum: *Phys.Lett.B* 464, 350–350 (1999)], [hep-ph/9812378](#).

[27] G. J. Gounaris, P. I. Porfyriadis, and F. M. Renard, *Eur. Phys. J. C* **9** (1999) 673–686, [hep-ph/9902230](#).

[28] D. Bardin, L. Kalinovskaya, V. Kolesnikov, and E. Uglov, “Light-by-light scattering in SANC”, in *International School-Workshop on Calculations for Modern and Future Colliders*, 11, 2006, [hep-ph/0611188](#).

[29] D. Bardin, L. Kalinovskaya, and E. Uglov, *Phys. Atom. Nucl.* **73** (2010) 1878–1888, [0911.5634](#).

[30] Z. Bern, A. De Freitas, L. J. Dixon, A. Ghinculov, and H. L. Wong, *JHEP* **11** (2001) 031, [hep-ph/0109079](#).

[31] T. Binoth, E. W. N. Glover, P. Marquard, and J. J. van der Bij, *JHEP* **05** (2002) 060, [hep-ph/0202266](#).

[32] A. A H, E. Chaubey, and H.-S. Shao, *JHEP* **03** (2024) 121, [2312.16966](#).

[33] A. A H, E. Chaubey, M. Fraaije, V. Hirschi, and H.-S. Shao, *Phys. Lett. B* **851** (2024) 138555, [2312.16956](#).

[34] J. H. Kuhn, E. Mirkes, and J. Steegborn, *Z. Phys. C* **57** (1993) 615–622.

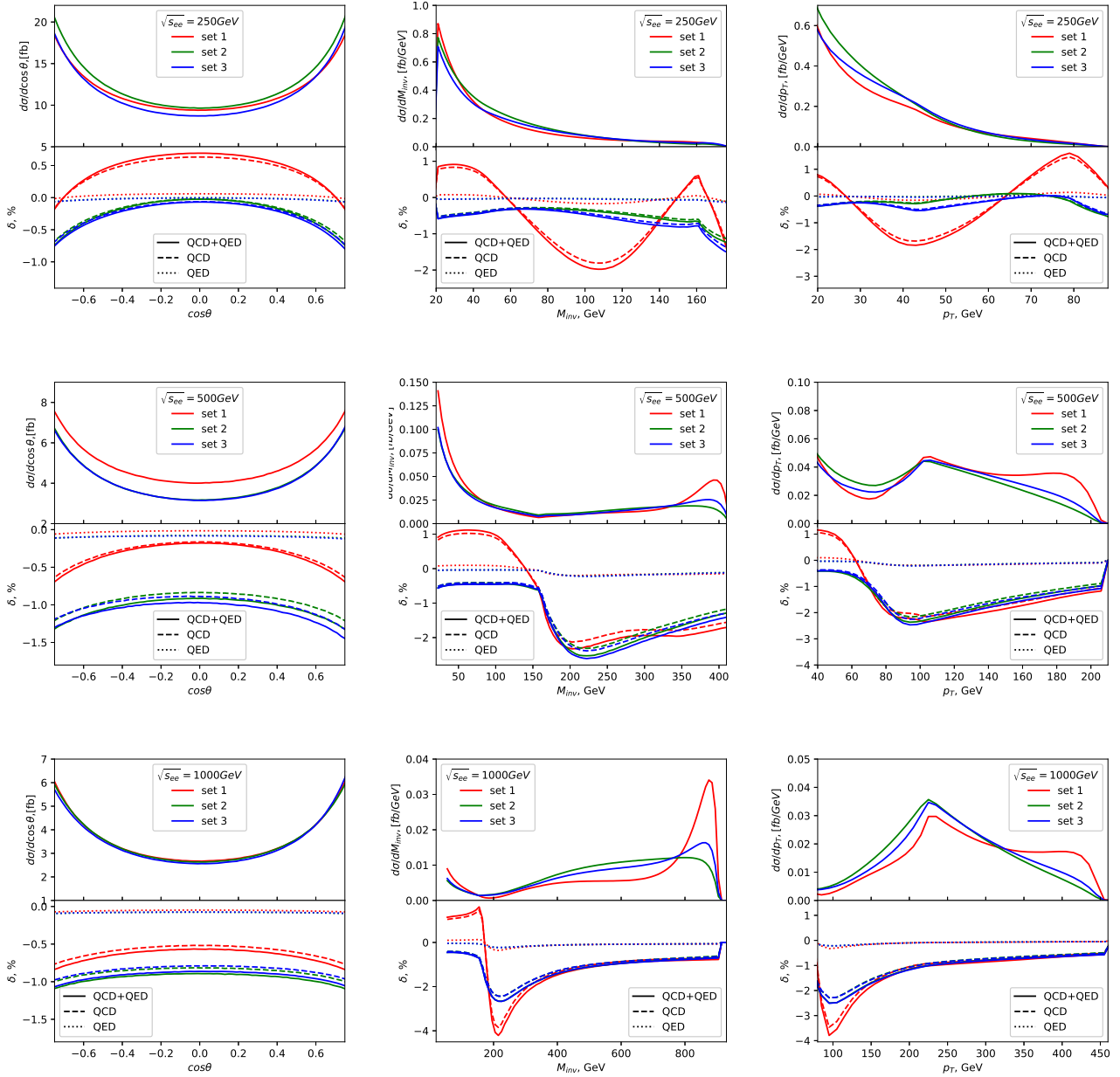


**Fig. 2.** Final state kinematic distributions of polarized LbL scattering at fixed incoming electron beam energies  $\sqrt{s_{ee}} = 250, 500$  and  $1000$  GeV and various polarization setups